

## ORIGINAL ARTICLE

# Mechanism-Based Modeling of Gastric Emptying Rate and Gallbladder Emptying in Response to Caloric Intake

B Guiastrennec<sup>1\*</sup>, DP Sonne<sup>2</sup>, M Hansen<sup>2,3</sup>, JI Bagger<sup>2</sup>, A Lund<sup>2</sup>, JF Rehfeld<sup>4</sup>, O Alskär<sup>1</sup>, MO Karlsson<sup>1</sup>, T Vilsbøll<sup>2</sup>, FK Knop<sup>2</sup> and M Bergstrand<sup>1</sup>

Bile acids released postprandially modify the rate and extent of absorption of lipophilic compounds. The present study aimed to predict gastric emptying (GE) rate and gallbladder emptying (GBE) patterns in response to caloric intake. A mechanism-based model for GE, cholecystokinin plasma concentrations, and GBE was developed on data from 33 patients with type 2 diabetes and 33 matched nondiabetic individuals who were administered various test drinks. A feedback action of the caloric content entering the proximal small intestine was identified for the rate of GE. The cholecystokinin concentrations were not predictive of GBE, and an alternative model linking the nutrients amount in the upper intestine to GBE was preferred. Relative to fats, the potency on GBE was 68% for proteins and 2.3% for carbohydrates. The model predictions were robust across a broad range of nutritional content and may potentially be used to predict postprandial changes in drug absorption.

CPT Pharmacometrics Syst. Pharmacol. (2016) 5, 692–700; doi:10.1002/psp4.12152; published online 27 December 2016.

### Study Highlights

#### WHAT IS THE CURRENT KNOWLEDGE ON THE TOPIC?

☑ Gastric emptying is accompanied by a strong increase in pH and bile acids concentration in the gastrointestinal tract, which may affect the solubility of orally administered drugs. These physiological processes are subject to a large variability, which can be challenging for the prediction of the rate and extent of drug absorption.

#### WHAT QUESTION DID THIS STUDY ADDRESS?

☑ How does nutritional content impact gastric emptying rate and gallbladder emptying and what are the influential factors of these processes?

#### WHAT THIS STUDY ADDS TO OUR KNOWLEDGE

☑ The model describes the complex relationship between the nutritional content of a test drink, the gastric emptying rate, and the change in gallbladder volume.

#### HOW MIGHT THIS CHANGE DRUG DISCOVERY, DEVELOPMENT, AND/OR THERAPEUTICS?

☑ The model could be utilized during drug development to predict postprandial changes in drug absorption. Gastric and gallbladder emptying are believed to play an important role in the development of diabetes; research within this field could be leveraged by the model predictions.

Absorption of orally administered drugs involves highly complex mechanisms.<sup>1</sup> The rate and extent of absorption for orally administered drugs are governed by the physiology of the gastrointestinal (GI) tract, the characteristics of the dosage form, and the physicochemical properties of the drug.<sup>1,2</sup>

The human GI tract comprises numerous organs dedicated to the processing of food for proper nutrient absorption.<sup>2,3</sup> These mechanisms are tightly coordinated by complex neural and hormonal pathways.<sup>4</sup> Changes in secretion volumes, pH, osmolality, and mechanical stress occur all along the GI tract and vary between the fasting and postprandial states.<sup>3</sup> In the fasting state, the secretory volumes are reduced, the pH is acidic in the stomach, and alkaline in the small intestine (SI).<sup>3</sup> In the postprandial state, fasting pH values are altered by the presence of food and an increase of the secretory volumes of saliva, gastric, and bile juices occurs.<sup>3,5</sup> Food entering the stomach is homogenized by the combined actions of enzymes and contractions of the stomach wall. The release of homogenized food (i.e., chyme) from the stomach is controlled by the rate of gastric emptying (GE), tightly regulating

the caloric delivery to the SI.<sup>6</sup> Upon entry into the SI, the chyme triggers the release of cholecystokinin (CCK), a gut hormone involved in the regulations of pancreatic enzyme secretion, intestinal motility, satiety signaling, and the inhibition of the gastric juice secretions.<sup>7,8</sup> The postprandial CCK elevation also stimulates gallbladder contractions and the subsequent flow of bile into the intestinal lumen.<sup>4,8</sup>

While for most drugs the characteristics of the dosage form are tailored to minimize the absorption variability *in vivo*, the physicochemical properties of a given drug are of major importance to predict the *in vivo* absorption behavior.<sup>9</sup> Accordingly, Amidon *et al.* established the biopharmaceutical classification system (BCS) to divide pharmaceutical compounds into four classes based on their solubility and their GI permeability.<sup>1</sup> Lipophilic compounds referred to as BCS class II (high permeability) and IV (low permeability) exhibit a low bioavailability in the fasting state. The bioavailability of these compounds can be improved by enabled formulations or concomitant administration of food.<sup>10</sup> As a BCS class I (high

<sup>1</sup>Department of Pharmaceutical Biosciences, Uppsala University, Uppsala, Sweden; <sup>2</sup>Center for Diabetes Research, Department of Medicine, Gentofte Hospital, University of Copenhagen, Hellerup, Denmark; <sup>3</sup>Current workplace: Novo Nordisk A/S, Bagsværd, Denmark; <sup>4</sup>Department of Clinical Biochemistry, Rigshospitalet, University of Copenhagen, Copenhagen, Denmark. \*Correspondence to: B Guiastrennec ([guiastrennec@gmail.com](mailto:guiastrennec@gmail.com))

Received 18 August 2016; accepted 24 October 2016; published online on 27 December 2016. doi:10.1002/psp4.12152

**Table 1** Subject demographics and clinical study designs

Characteristics	Study A	Study B	Study C	Study D
Reference	Hansen <i>et al.</i> <sup>18</sup>	Bagger <i>et al.</i> <sup>19</sup>	Sonne <i>et al.</i> <sup>17</sup>	Sonne <i>et al.</i> <sup>20</sup>
Test drink type	water	3 glucose based	1 glucose + 3 fat based	1 fat based
N (patients/healthy)	10/10	8/8	15/15	0/10
Medical condition	T2D	T2D	T2D	none
Sex (male/female)	16/4	6/10	18/12	5/5
Age (years)	62 (44–74)	57 (38–75)	60 (42–71)	48 (29–66)
Weight (kg)	89.9 (69.5–113)	89.6 (67.0–122)	86.2 (63.6–122)	78 (68–90)
Height (m)	1.78 (1.64–1.89)	1.75 (1.61–1.92)	1.76 (1.58–1.97)	1.75 (1.62–1.90)
BMI (kg/m <sup>2</sup> )	28.5 (24.3–35.0)	29.2 (25.2–34.1)	27.9 (24.0–31.9)	24.1 (21.2–27.1)
Assessment times (min)	Acetaminophen 0, 5, 10, 20, 30, 40, 50, 60, 90, 120, 150, 180	Acetaminophen 0, 10, 20, 30, 45, 60, 75, 90, 120, 180, 240	Acetaminophen -20, -10, 0, 15, 30, 45, 60, 90, 120, 180, 240 CCK -20, -10, 0, 15, 30, 45, 60, 90, 120, 180 Gallbladder volume -10, 0, 10, 20, 30, 40, 50, 60	Acetaminophen, CCK -20, -10, 0, 5, 10, 20, 30, 40, 50, 60, 75, 90, 105, 120, 150, 180, 210, 240

Continuous variables given as mean (range). BMI, body mass index; CCK, cholecystokinin; T2D, Type 2 diabetes.

solubility, high permeability), acetaminophen (i.e., paracetamol) is not absorbed through the stomach wall, whereas it is extensively absorbed in the SI.<sup>10,11</sup> The GE rate is therefore the rate-limiting step in the absorption of acetaminophen and can be indirectly evaluated through the appearance rate of acetaminophen in the circulation.<sup>12,13</sup>

Postprandially, the absorption of lipophilic compounds can be affected in different ways depending on their physicochemical properties and the composition of the meal.<sup>2,10</sup> The postprandial effect is maximized by the presence of fats, potent stimulators of gallbladder emptying (GBE), and subsequent bile flow into the SI.<sup>5,14,15</sup> The amount of bile released postprandially can improve the absorption of the lipophilic compound through the solubilizing action of bile acids; these processes are, however, highly variable.<sup>2,10,16</sup>

Accurate prediction of the rate and extent of absorption of lipophilic compounds relies on the capacity to predict the GE rate and GBE in the fasting and in the postprandial states. Nonlinear mixed effects (NLME) models have demonstrated their utility in the prediction of complex dynamic systems.<sup>16</sup> In the present study we investigated the effects of various caloric intake on the GE rate, plasma CCK concentrations, and GBE through an NLME modeling approach.

## METHODS

### Study design

Data from three previously published clinical studies were pooled and used for the model development (Table 1, Study A–C).<sup>17–19</sup> An additional study was used for the external validation of the GE and CCK models (Table 1, Study D).<sup>20</sup> All clinical studies were approved by the scientific-ethical committee of the Capital Region of Denmark and conducted according to the principles of the Helsinki Declaration II.

**Model development dataset.** This dataset included data from 33 subjects with type 2 diabetes (T2D) and 33

nondiabetic control individuals matched with respect to gender, age, and body mass index (BMI). In a crossover study design, subjects were administered water (Study A), three different glucose solutions (Study B), or isocaloric test drinks with low, medium, and high fat (Study C) content (Table 2) after an overnight (10 h) fast. In Study A, the dose was administered directly to the stomach within 1 m through a nasogastric feeding tube. Each test drink contained dissolved acetaminophen (1.5 g) to assess the rate of GE. Acetaminophen was assumed to empty from the stomach at the same rate as the nutrients. Acetaminophen plasma concentrations were collected repeatedly for up to 4 h following test drink administration. Additionally, in Study C, CCK plasma concentrations and ultrasound assessments of gallbladder volume were regularly measured, over periods of 3 h and 1 h, respectively (Table 1).

**External validation dataset.** This dataset (Study D) included data from 10 nondiabetic control individuals. Subjects were given acetaminophen (1.5 g) dissolved in a medium-high fat content test drink (Table 2) after a 10-h overnight fast. Acetaminophen plasma concentrations were collected for 4 h after test drink administration (Table 1).

### Parameter estimation and model selection

The data analysis was performed using an NLME modeling (NONMEM v. 7.3) approach aided by functionalities of the PsN toolkit (v. 4.4.2).<sup>21</sup> The first-order conditional estimation method with interaction and the ADVAN13 subroutine were used for parameter estimation. Model selection was based on changes in the objective function value (OFV), with a significance level of  $P < 0.05$ . Graphical diagnostics, physiological plausibility, and uncertainty were also considered in the model evaluation. Parameter uncertainty expressed as relative standard error (RSE) was obtained from the NONMEM sandwich estimator computed with an importance sampling step. Visual predictive checks (VPC) stratified by test drink were used throughout model

**Table 2** Test drink properties

Characteristics	Study A	Study B			Study C				Study D
	Water	OGTT 25 g	OGTT 75 g	OGTT 125 g	OGTT 75 g	Low fat	Medium fat	High fat	Medium-high fat
Volume (mL)	100	300	300	300	300	350	350	350	350
Carbohydrate (g)	0	25	75	125	75	107	93	32	58
Protein (g)	0	0	0	0	0	13	11	3	10
Fat (g)	0	0	0	0	0	2.5	10	40	28
Energy (kcal)	0	100	300	500	300	502.5	506	500	524

OGTT, oral glucose tolerance test.

development for evaluation of models predictive performances.<sup>22</sup> All VPC were created by simulating 1,000 datasets and deriving the 95% confidence intervals around the 5th, 50th, and 95th percentiles of the observations and predictions. The predictive performance of the GE model was further evaluated based on VPC of the external validation dataset.

Summary statistics of the time to empty 50% of the stomach content ( $T_{GE50}$ ) and the gallbladder ejection fraction (EF%) (Eq. 1) were calculated on 1,000 simulations of the model development dataset and summarized by deriving a range of prediction intervals (PI)<sup>17</sup>:

$$EF\% = \frac{GVol_0 - GVol}{GVol_0} \cdot 100 \quad (1)$$

where  $GVol$  is the gallbladder volume at any timepoint and  $GVol_0$  is the gallbladder volume at baseline.

### Model development

The models for GE, plasma CCK and GBE were developed in a stepwise manner. The GE model was first developed, validated, and subsequently used to predict the individual GE rates. The latter were utilized in the CCK and GBE models via an individual pharmacokinetic parameters with standard errors (IPPSE) approach. IPPSE was selected in order to handle imprecisions in the estimates of individual GE parameters.<sup>23</sup>

**GE model.** Published population models were used for the description of acetaminophen (GE marker) pharmacokinetics.<sup>24–26</sup> The disposition was described by a two-compartment model with first-order elimination (CL).<sup>25,26</sup> Acetaminophen was absorbed from an upper SI compartment after being emptied from the stomach compartment.<sup>24,25</sup> The distinction between the absorption rate constant ( $K_A$ ) and the GE rate constant ( $K_G$ ) was not possible with the current study design. In a previously published study, acetaminophen was administered along with a nonabsorbable isotopic marker intended to measure GE rate and thus allowing to properly distinguish the  $K_A$  from the  $K_G$ .<sup>11</sup> The reported half-life of  $K_A$  ( $6.8 \pm 0.9$  min, mean  $\pm$  SE) was implemented in the model as a frequentist prior.<sup>11,27</sup> The postprandial effect on the GE rate was implemented using a feedback loop from the caloric content of the upper SI.<sup>28</sup> The caloric content of test drink was derived from the amount of fats (9 kcal/g), proteins (4 kcal/g), and carbohydrates (4 kcal/g)<sup>29</sup>. The nature of the feedback mechanism was investigated

using linear and nonlinear ( $E_{max}$  and sigmoidal) functions. The effect of ingested volume on GE could not be conclusively investigated due to the limited range of tested volumes. The dose infusion rate into the stomach was fixed to 1 min for Study A and set as bolus input for all other studies. Delays in the initial phase of GE were evaluated on all test drinks with a lag-time and an onset function.<sup>30</sup> The residence time of the nutrients in the upper SI was mediated by  $K_{UL}$  the transfer rate constant between upper and lower SI. The presence of a saturable metabolic first-pass for acetaminophen was evaluated using an  $E_{max}$ -type function. A saturable absorption of nutrients from the upper SI was added to the model and parameters were fixed to published values for glucose.<sup>24</sup> Sensitivity analyses were performed on the  $K_A$  and the saturable absorption parameters by shifting them to  $\pm 25$  and  $\pm 50\%$  and quantifying changes in parameter estimates.

**CCK model.** Postprandial plasma CCK concentrations showed two peaks.<sup>17,20</sup> The first peak was high and narrow, whereas the second peak was lower and wider. The peaks are referred to as fast ( $CCK_F$ ) and late ( $CCK_L$ ) secretion of CCK, respectively. Two indirect response models were used to describe the changes in plasma  $CCK_F$  and  $CCK_L$  concentrations. A postprandial effect was implemented via the stimulation of the rate of CCK production  $R_{prodF}$  and  $R_{prodL}$ . Precursor pools were tested on each indirect response model to mimic exhaustion of the secretion process.<sup>31</sup> With the precursor pools the postprandial effect was implemented as an increase in the rate constant of release from the pool into the plasma ( $K_{RF}$  and  $K_{RL}$ ). The effect on CCK secretion was tested through linear and nonlinear ( $E_{MAX}$  and sigmoidal) functions of the amount of nutrients in duodenum for  $CCK_F$  and upper jejunum for  $CCK_L$ .<sup>7</sup> The relative potency of proteins and carbohydrates to trigger the release of CCK were evaluated with regard to fats.<sup>32</sup> Nutrients in the duodenum and upper jejunum were nonlinearly absorbed as described for the GE model.<sup>24</sup> Assuming similar volume of distribution, the total plasma CCK concentrations were obtained by summing the predicted concentrations of  $CCK_F$  and  $CCK_L$ .

**GBE model.** The time course of gallbladder volume was modeled by an indirect response model where the emptying was caused by an increase in the emptying rate constant  $K_{RB}$ . Two alternative emptying mechanisms were tested; GBE was either driven 1) by the predicted plasma CCK concentrations, or 2) by a signal of the nutrients in the upper SI.<sup>15</sup> In both alternatives, the increase in  $K_{RB}$  was

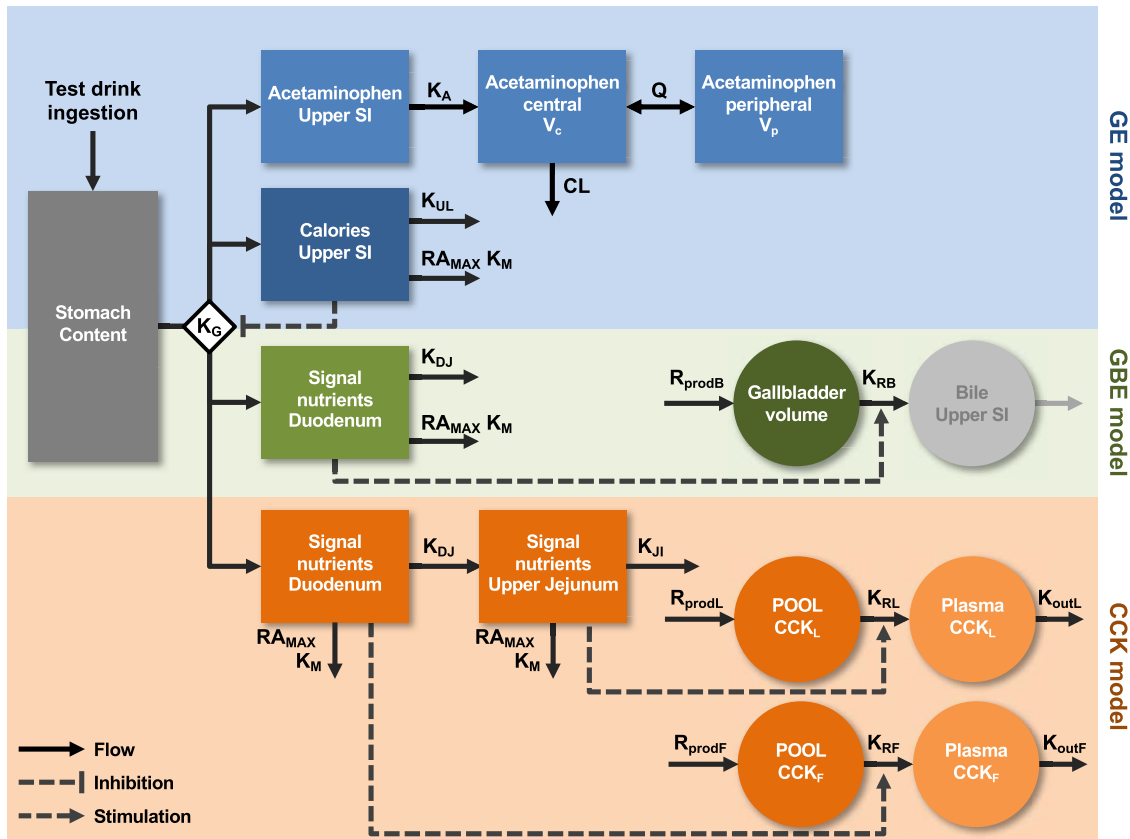


**Figure 1** Schematic representation of the selected gastric emptying (GE, blue), cholecystikinin (CCK, orange), and gallbladder emptying (GBE, green) models structure. The test drink was administered to the stomach (dark gray). The GE was governed by the rate constant  $K_G$ , which was inhibited by calories in the upper small intestine (SI) (dark blue).  $K_{UL}$  was the rate constant of calories disappearance from the upper SI,  $K_{DJ}$  from the duodenum, and  $K_{JI}$  from the upper jejunum. Nutrients and calories also disappeared in a nonlinear manner,  $RA_{MAX}$  describing the maximal rate of their absorption and  $K_M$  the potency of their absorption. The acetaminophen model (light blue) was characterized by the absorption rate constant ( $K_A$ ), the clearance ( $CL$ ), central ( $V_C$ ), and peripheral volumes ( $V_P$ ) of distribution and intercompartmental clearance ( $Q$ ). The gallbladder volume compartment (dark green) was characterized by a production rate ( $R_{prodB}$ ) and a release rate constant ( $K_{RB}$ ). Nutrients in the duodenum would generate a signal that increased  $K_{RB}$  and releasing bile into the upper SI (light gray, compartment added for illustration purpose). Likewise, nutrients in the duodenum and upper jejunum would generate a signal that respectively released the  $CCK_F$  and  $CCK_L$  from the pools. Production of  $CCK_F$  and  $CCK_L$  were mediated by the rates  $R_{prodF}$  and  $R_{prodL}$ . The release from the pools to the plasma was controlled by the release rate constant  $K_{RF}$  and  $K_{RL}$ , on which the nutrient signal would act. Finally, the disappearance of CCK from the plasma was controlled by the disappearance rate constants  $K_{outF}$  and  $K_{outL}$ .

tested through linear and nonlinear ( $E_{MAX}$  and sigmoidal) functions of the emptying signal. For the second alternative, the relative potency of proteins and carbohydrates to trigger GBE were estimated with regard to fats.<sup>15</sup> With the second alternative, the nutrients in duodenum were nonlinearly absorbed as described previously for the GE model.<sup>24</sup> Recirculation of the emptied bile from the SI to the gallbladder was also investigated using a chain-of-transit compartments.<sup>33</sup>

**Covariate analysis**

The GE rate has been reported to be mainly influenced by gender, obesity, and diseases such as T2D.<sup>34–37</sup> Hence, these effects were investigated on key structural parameters related to GE. For CCK and GBE, physiologically plausible effects of age, gender, body weight (WT), BMI, and T2D were evaluated on structural parameters. Covariates selection was performed through a stepwise covariate

modeling (SCM) approach with forward inclusion ( $P < 0.05$ ) and backward deletion ( $P < 0.01$ ) steps. Continuous covariates were parameterized using linear effects.

**Stochastic models**

Subjects studied over several crossover occasions were assumed to be independent individuals throughout the analysis. Between subject variability (BSV) was evaluated on key structural model parameters using a log-normal distribution. Proportional, additive, and combined models were tested for the residual unexplained variability (RUV).

**RESULTS**

A schematic representation of the selected GE, CCK and GBE models is provided in **Figure 1**. Parameter estimates for the selected model are reported in **Table 3**; the model

**Table 3** Selected models parameter estimates

Gastric emptying model			Cholecystokinin model			Gallbladder emptying model		
Parameters (unit)	Estimates (RSE%)	BSV CV% (RSE%)	Parameters (unit)	Estimates (RSE%)	BSV CV% (RSE%)	Parameters (unit)	Estimates (RSE%)	BSV CV% (RSE%)
CL/F (L/min)	0.441 (2.5)		BASE <sub>CCKF</sub> (pM)	0.506 (11)	58 (42)	BASE <sub>BILE</sub> (mL)	36.3 (2.5)	27 (11)
V <sub>o</sub> /F (L)	19.5 (12)	68 (32)	BASE <sub>CCKL</sub> (pM)	0.0882 (125)		K <sub>RB</sub> (min <sup>-1</sup> )	0.0618 (13)	90 (29)
V <sub>p</sub> /F (L)	48.1 (4.4)		POOL <sub>CCKF</sub> (pM)	17.1 (6.9)		S <sub>MAX-BILE</sub>	6.62 (12)	
Q/F (L/min)	1.56 (5.6)		POOL <sub>CCKL</sub> (pM)	1.95 (11)	42 (21)	S <sub>50-BILE</sub>	5.52 (20)	80 (15)
F <sub>1</sub>	1 fixed	22 (12)	K <sub>ouIF</sub> (min <sup>-1</sup> )	0.355 (8.1)	72 (25)	K <sub>DJ</sub> (min <sup>-1</sup> )	0.0833 fixed	
HL-K <sub>A</sub> <sup>a</sup> (min)	8.19 (8.6)		K <sub>ouIL</sub> (min <sup>-1</sup> )	0.00546 (21)		RA <sub>MAX</sub>	2.292 fixed	
K <sub>G0</sub> (min <sup>-1</sup> )	1.06 (21)	155 (17)	S <sub>MAX-CCKF</sub>	0.193 (18)		K <sub>M</sub> (kcal)	25.12 fixed	
K <sub>UL</sub> (min <sup>-1</sup> )	0.0266 (10)	56 (21)	S <sub>50-CCKF</sub>	0.592 (82)		POT <sub>fatB</sub> (%)	100 fixed	
RA <sub>MAX</sub>	2.292 fixed		SLP <sub>CCKL</sub>	0.0377 (54)		POT <sub>protB</sub> (%)	67.9 (26)	
K <sub>M</sub> (kcal)	25.12 fixed		K <sub>DJ</sub> (min <sup>-1</sup> )	0.0833 fixed		POT <sub>carbB</sub> (%)	2.25 (22)	
SLP <sub>CAL</sub>	-0.0173 (8.8)	19 (31)	K <sub>JL</sub> (min <sup>-1</sup> )	0.0111 fixed		WT-BASE <sub>BILE</sub> (%/kg)	+1.19 (13)	
SIG	0.285 (17)		RA <sub>MAX</sub>	2.292 fixed		AGE-S <sub>50-BILE</sub> (%/year)	+2.15 (21)	
T <sub>50OGTT</sub> (min)	15.7 (13)		K <sub>M</sub> (kcal)	25.12 fixed		Add. Err. (mL)	2.33 (12)	
T <sub>50Fat</sub> (min)	23.1 (13)		POT <sub>fatC</sub> (%)	100 fixed		Prop. Err. (%)	7.66 (19)	
SEX-SLP <sub>CAL</sub> (%)	+40.7 (18)		POT <sub>protC</sub> (%)	0 fixed				
Prop. Err. (%)	14.8 (2.3)		POT <sub>carbC</sub> (%)	10.1 (65)		<i>Derived parameters<sup>b</sup></i>		
			T2D-POT <sub>carbC</sub> (%)	-81.1 (6.5)		R <sub>prodB</sub> (mL/min)	2.24	
			Prop. Err. (%)	29.5 (32)				
			<i>Derived parameters<sup>b</sup></i>					
			R <sub>prodF</sub> (pM/min)	0.180				
			R <sub>prodL</sub> (pM/min)	0.000482				
			K <sub>RF</sub> (min <sup>-1</sup> )	0.0105				
			K <sub>RL</sub> (min <sup>-1</sup> )	0.000247				

Add. Err, additive part of the residual unexplained variability; AGE-S<sub>50-BILE</sub>, effect of age on S<sub>50-BILE</sub>; BASE<sub>BILE</sub>, baseline gallbladder volume; BASE<sub>CCKF</sub> and BASE<sub>CCKL</sub>, baseline plasma concentrations of CCK<sub>F</sub> and CCK<sub>L</sub>; BSV, between subject variability; CL/F, apparent acetaminophen clearance; CV, coefficient of variation; F<sub>1</sub>, relative acetaminophen bioavailability; HL-K<sub>A</sub>, half-life of the acetaminophen absorption rate; K<sub>DJ</sub>, nutrient transfer rate constant between duodenum and jejunum; K<sub>G0</sub>, baseline gastric emptying rate constant; K<sub>M</sub>, potency of caloric absorption; K<sub>JL</sub>, nutrient transfer rate constant between upper and lower jejunum; K<sub>ouIF</sub>, K<sub>ouIL</sub>, the CCK<sub>F</sub> and CCK<sub>L</sub> plasma disappearance rate constant; K<sub>RB</sub>, gallbladder emptying rate constant; K<sub>RF</sub>, CCK<sub>F</sub> pool emptying rate constant calculated as R<sub>prodF</sub>/POOL<sub>CCKF</sub>; K<sub>RL</sub>, CCK<sub>L</sub> pool emptying rate constant calculated as R<sub>prodL</sub>/POOL<sub>CCKL</sub>; K<sub>UL</sub>, nutrients transfer rate constant between upper and lower small intestine; POOL<sub>CCKF</sub>, POOL<sub>CCKL</sub>, pool size of CCK<sub>F</sub> and CCK<sub>L</sub>; POT<sub>carbB</sub>, POT<sub>fatB</sub>, POT<sub>protB</sub>, relative potency of carbohydrates, fats, and proteins on gallbladder emptying; POT<sub>carbC</sub>, POT<sub>fatC</sub>, POT<sub>protC</sub>, relative potency of carbohydrates, fats, and proteins on the release of CCK; Prop. Err., proportional part of the residual unexplained variability; Q/F, apparent acetaminophen inter-compartmental clearance; RA<sub>MAX</sub>, maximal nutrients absorption rate; R<sub>prodB</sub>, rate of bile production calculated as BASE<sub>BILE</sub> x K<sub>RB</sub>; R<sub>prodF</sub>, rate of CCK<sub>F</sub> production calculated as BASE<sub>CCKF</sub> x K<sub>ouIF</sub>; R<sub>prodL</sub>, rate of CCK<sub>L</sub> production calculated as BASE<sub>CCKL</sub> x K<sub>ouIL</sub>; RSE, relative standard error; S<sub>50-BILE</sub>, nutrients signal leading to 50% effect of S<sub>MAX-BILE</sub>; S<sub>50-CCKF</sub> signal leading to 50% effect of S<sub>MAX-CCKF</sub>; SEX-SLP<sub>CAL</sub>, effect of gender on SLP<sub>CAL</sub>; SIG, sigmoidicity factor of the gastric emptying onset; SLP<sub>CAL</sub>, slope of the caloric feedback loop on gastric emptying; SLP<sub>CCKL</sub>, slope of the nutrients signal effect on release of CCK<sub>L</sub>; S<sub>MAX-BILE</sub>, maximal gallbladder emptying effect; S<sub>MAX-CCKF</sub>, maximal secretion effect on CCK<sub>F</sub>; T2D-POT<sub>carbC</sub>, effect of type 2 diabetes on POT<sub>carbC</sub>; T<sub>50OGTT</sub> and T<sub>50Fat</sub>, time to 50% of maximal gastric emptying onset for carbohydrate and fat based test drink; V<sub>o</sub>/F and V<sub>p</sub>/F, apparent acetaminophen central and peripheral volumes of distribution; WT-BASE<sub>BILE</sub>, effect of body weight on BASE<sub>BILE</sub>.

<sup>a</sup>Parameter with prior information (HL-K<sub>A</sub><sub>prior</sub> = 6.8 ± 0.9 min).

<sup>b</sup>Typical parameter value not estimated but derived from other estimated parameters.

code for GE–GBE can be found in **Supplementary Material S1** and a table of parameter shrinkages in **Supplementary Material S2**.

### GE model

In total, 183 individual profiles and 1,615 acetaminophen concentrations all above the lower limit of quantification (LLOQ = 0.001 mM) were used for the model development. One subject missed the acetaminophen dose over all studied occasions and was therefore excluded from the analysis. The estimated half-life of the basal GE rate K<sub>G0</sub> was short (0.66 min) and highly variable BSV of 155%. The postprandial effect on the GE rate was best described by a

linear feedback of the caloric content in the upper SI on K<sub>G0</sub> (Eq. 2):

$$K_G = K_{G0} \cdot (1 - SLP_{CAL} \cdot CAL_{USI}) \quad (2)$$

where SLP<sub>CAL</sub> represents the slope of the linear feedback and CAL<sub>USI</sub> the caloric content in the upper SI. Delays in the initial phase of GE were added for the glucose solutions (OGTT) and the fat-based test drinks resulting in significant improvements of the model fit. The GE onset function (Eq. 3) gave better performance and stability (i.e., no change point) over a lag-time; further improvements in the initial phase of GBE were also noted:

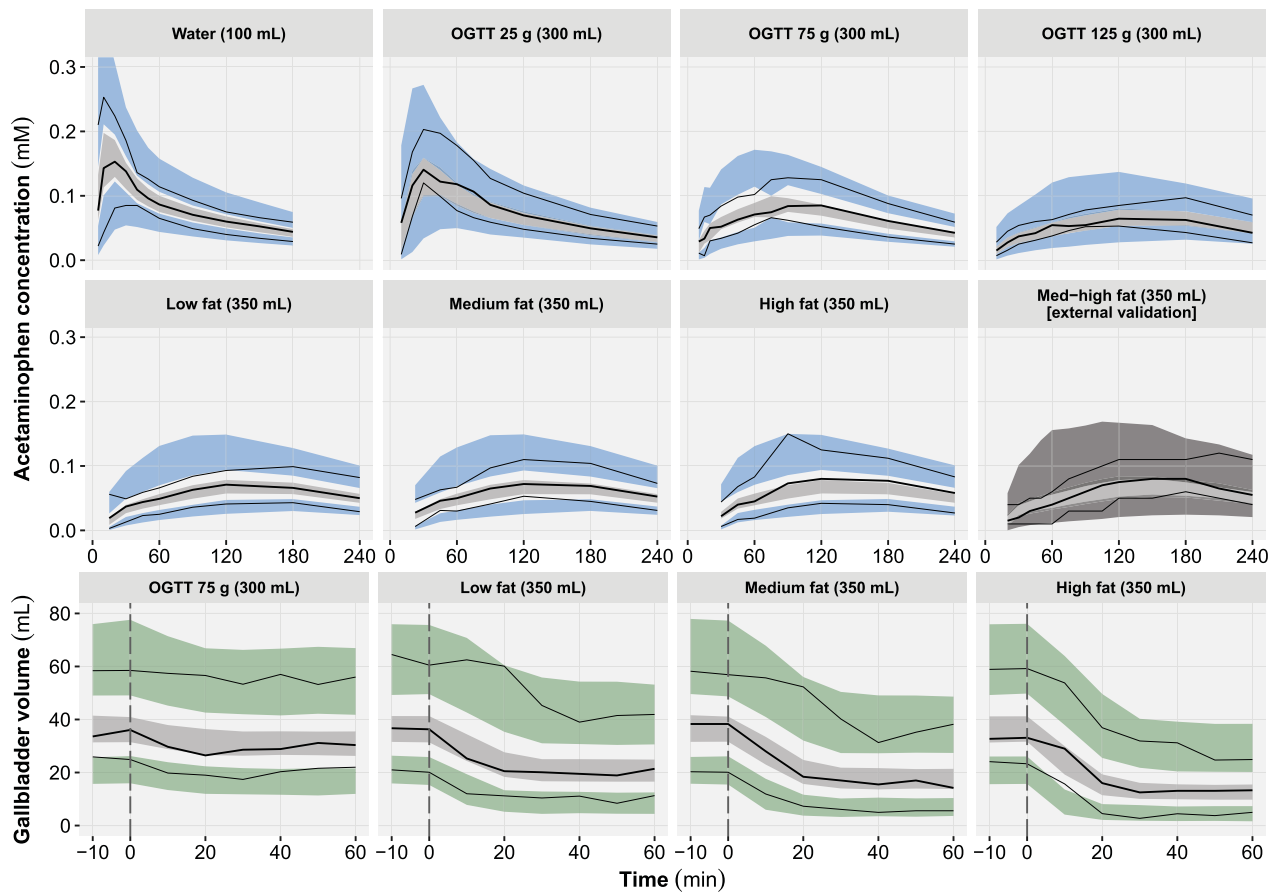


**Figure 2** Visual predictive checks of the acetaminophen plasma concentration (top) and gallbladder volume (bottom) time course and stratified by test drink. For each panel, the median (bold lines), 5th and 95th percentiles (thin lines) of the observed data are compared to the 95% confidence intervals (shaded areas) for the median (light gray), 5th and 95th percentiles of the simulated data (blue/dark gray: acetaminophen, green: gallbladder volume) (based on 1,000 simulations). The external validation of acetaminophen was performed by simulation only. The vertical lines (dashed gray) represent the time of the test drink administration. OGTT, oral glucose tolerance test.

$$GE_{onset} = \frac{1}{1 + e^{-SIG \cdot (TAD - T_{50})}} \quad (3)$$

where SIG represents the sigmoidicity factor of the onset, TAD the time after the last dose, and  $T_{50}$  the time to 50% of the maximal onset. Estimating the variability in the relative bioavailability of acetaminophen was significant, whereas a saturable first-pass did not lead to further improvement of the model fit and was not retained in the selected model.

The sensitivity analyses of the  $K_A$  and the saturable nutrient absorption parameters revealed only small changes in model fit and typical parameter estimates (within  $\pm 20\%$ ), with the exception of the typical value of  $V_C$  and its BSV for  $K_A$  which were inversely correlated with the changes in  $K_A$  and  $K_{UL}$ , which was inversely correlated with changes in the maximal absorption rate ( $RA_{max}$ ). The SCM revealed a significantly stronger feedback (+40%,  $P < 0.001$ ) of the calories in the upper SI on GE rate ( $SLP_{CAL}$ ) in females than in males (Eq. 4):

$$SLP_{CAL_i} = TVSLP_{CAL} \cdot (1 + 0.4 \cdot FEM_i) \cdot \exp(\eta_i) \quad (4)$$

where FEM is a flag of value 1 for females and 0 for males, and  $\eta_i$  the BSV for  $SLP_{CAL}$  of subject  $i$ . The RUV of GE was best described with a proportional error model. VPC of the selected GE model with the external validation is provided in **Figure 2**. The simulation-based  $T_{GE50}$  for the studied population (no gender distinction) ranged from 3.8 min ( $PI_{95}$ : 0.2–15 min) for water and up to 96 min ( $PI_{95}$ : 64–133 min) for a high-fat test drink. Detailed simulation-based  $T_{GE50}$  stratified by drink content and gender are provided in **Figure 3**.

### CCK model

In total, 115 individual profiles and 1,150 CCK plasma concentrations all above the LLOQ (0.1 pM) were used for the model development. The model predictions were improved by the use of precursor pools for both  $CCK_F$  and  $CCK_L$ . The baselines and the estimated pool sizes were markedly bigger for  $CCK_F$  ( $BASE_{CCKF} = 0.506$  pM,  $POOL_{CCKF} = 17.1$  pM) than  $CCK_L$  ( $BASE_{CCKL} = 0.0882$  pM,  $POOL_{CCKL} = 1.95$  pM). The opposite trend was observed with the respective estimated half-lives of 1.95 min and 127 min for  $CCK_F$  and  $CCK_L$ , respectively. Both the nutrients transfer rate

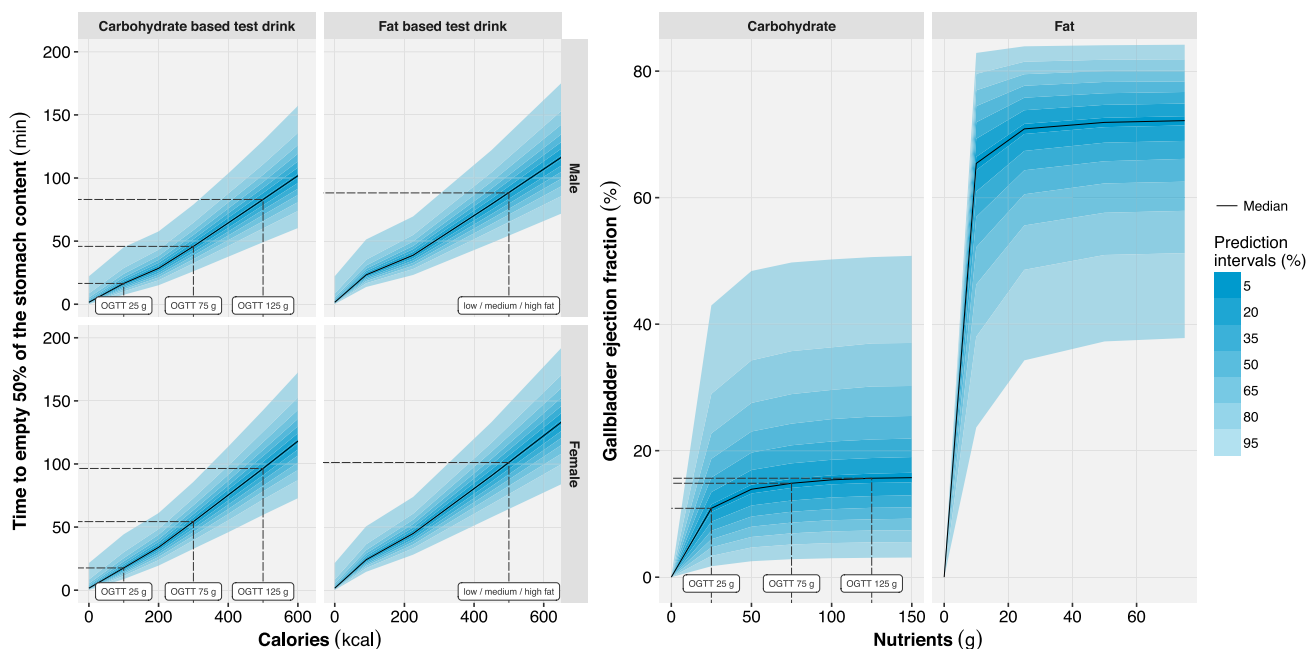


**Figure 3** *Left*: model-based simulations of the time to empty 50% of the stomach content ( $T_{GE50}$ ) vs. caloric content stratified by gender and test drink composition. *Right*: model-based simulations of the gallbladder ejection fraction vs. the amount of nutrients (differentiation is made between carbohydrates and fats). For each panel different prediction intervals (shaded areas) and the median (solid lines) were calculated based on 1,000 simulations of the development dataset. Dashed lines were added to denote the median  $T_{50GE}$  (*left*) and median gallbladder ejection fraction (*right*) of the studied test drinks (labels). OGTT, oral glucose tolerance test.

between duodenum and jejunum ( $K_{DJ}$ ) as well as the nutrients transfer rate between upper and lower jejunum ( $K_{JI}$ ) were poorly estimated (i.e., high RSE) and were later fixed to previously published values ( $K_{DJ} = 0.0833 \text{ min}^{-1}$  and  $K_{JI} = 0.0111 \text{ min}^{-1}$ ).<sup>24</sup> The release of  $CCK_F$  was nonlinearly correlated with the signal of nutrients in duodenum as opposed to the release of  $CCK_L$ , where a linear model of the amount of nutrients in the upper jejunum was more appropriate. In comparison to fats, the potency of carbohydrates to stimulate  $CCK$  secretion was noticeably lower ( $POT_{carbC} = 10\%$ ), whereas the potency of proteins ( $POT_{protC}$ ) was not supported in the model. In addition,  $POT_{carbC}$  was found to be significantly impaired ( $-81\%$ ,  $P < 0.001$ ) in patients with T2D compared to nondiabetic individuals (Eq. 5):

$$Signal_{nutrients} = g_{fat} \cdot POT_{fatC} + g_{carb} \cdot POT_{carbC} \cdot (1 - 0.811 \cdot T2D) \quad (5)$$

where  $g_{fat}$  and  $g_{carb}$  are the amount of fats and carbohydrates in either duodenum or upper jejunum, T2D is a flag set to 0 for nondiabetic individuals and 1 for patients with T2D. Several parameters such as  $BASE_{CCKL}$  (125% RSE),  $POT_{carbC}$  (65% RSE), and the signal-effect related parameters for the secretion of  $CCK_F$  (RSE  $S_{50-CCKF} = 82\%$ ) and  $CCK_L$  (RSE  $SLP_{CCKL} = 54\%$ ) were poorly estimated. The RUV of  $CCK$  was best described with a proportional error model. VPC of the selected  $CCK$  model is provided in **Supplementary Material S3**.

#### GBE model

In total, 115 individual profiles and 920 gallbladder volume measurements all above the LLOQ (5 mL) were used for

the model development. When the predicted plasma  $CCK$  concentrations were used as driver of the GBE, the model poorly predicted the data (**Supplementary Material S4**). However, when the signal of the nutrients in the duodenum was used instead, the kinetics of GBE was properly predicted by the model (**Figure 2**). An  $E_{max}$  type model best described the relationship between GBE and the signal generated by nutrients in duodenum. In relation to fats (100%), the potency of proteins (68%) and carbohydrates (2.3%) to trigger GBE was markedly lower (Eq. 6):

$$Signal_{nutrients} = g_{fat} \cdot POT_{fatB} + g_{carb} \cdot POT_{carbB} + g_{prot} \cdot POT_{protB} \quad (6)$$

where  $g_{fat}$ ,  $g_{carb}$ , and  $g_{prot}$  are the amounts of fats, carbohydrates, and proteins in the upper SI and  $POT_{fatB}$ ,  $POT_{carbB}$ , and  $POT_{protB}$  their relative potency. Recirculation of the emptied bile from the SI to the gallbladder was not supported by the data. The gallbladder size at baseline ( $BASE_{BILE}$ ) was positively correlated with WT ( $+1.19\%/kg$ ,  $P < 0.001$ ) (Eq. 7):

$$BASE_{BILE_i} = TVBASE_{BILE} \cdot (1 + 0.0119 \cdot (WT_i - 86)) \cdot \exp(\eta_i) \quad (7)$$

The nutrients generated signal leading to 50% of the maximal effect on GBE ( $S_{50-BILE}$ ) was positively correlated with age ( $+2.15\%/yr$ ,  $P < 0.01$ ) (Eq. 8):

$$S_{50-BILE_i} = TVS_{50-BILE} \cdot (1 + 0.0215 \cdot (AGE_i - 64)) \cdot \exp(\eta_i) \quad (8)$$

A combined model was selected to describe the RUV of GBE. The simulation-based gallbladder ejection fraction

was predicted to be up to 65% ( $PI_{95}$ : 37–82%) with a high-fat test drink (**Figure 3**).

## DISCUSSION

The developed model framework was demonstrated to be predictive of GE, plasma CCK, and GBE in response to caloric intake. The mechanism-based approach allowed prediction of a gradual transition between the fasting and the postprandial states. The significant variability observed in parameters governing the rate of GE and GBE (**Figure 3**) supports the hypothesis that a substantial fraction of the variability in the absorption of lipophilic compounds arises from variability in the GI tract.<sup>3</sup>

The simulation-based prediction of  $T_{GE50}$  for water (~3.8 min) was slightly shorter than the 5.2 min reported by Hens *et al.*<sup>38</sup> This discrepancy might be explained by differences in method, population demographic, and administered volume (i.e., 100 vs. 250 mL). In relative terms, the GE rate was found to be substantially variable under fasting condition (i.e., water only). However, under postprandial conditions this variability was dampened by the homeostatic feedback effect of caloric content in the SI on the rate of GE. In line with previous findings, GE was appropriately predicted by the caloric content in the upper SI independently of the nature of the nutrients (**Figure 2**).<sup>28,39</sup> While osmolality has also been suggested to play a role in the regulation of GE, this information was not available for the studied drinks.<sup>4</sup> A postprandial onset of GE was longer for fat- ( $T_{50Fat} = 23.1$  min) than for glucose- ( $T_{50OGTT} = 15.7$  min) based test drinks. Postprandial onsets of GE have previously been reported with both liquid and solid meals.<sup>11,40</sup> The addition of a compartment to account for an effect of stomach content volume on GE was not significant, which contrasts with previous research.<sup>28</sup> Although it is not excluded that the ingested volume acts on the GE rate, the current study design aimed to describe the effect of calories (0–506 kcal), but did not have the appropriate design to investigate an effect of ingested volume (100–350 mL). In line with previous publications, the postprandial GE was significantly impacted by gender (+40%) and moderately impacted by T2D (+10%), although the latter was removed from the selected model due to lack of significance.<sup>34,37</sup>

The secretion of CCK was mediated through a signal from nutrients in duodenum and upper jejunum where the CCK secreting cells (I cells) are concentrated (**Figure 1**).<sup>7</sup> The use of precursor models along with an effect of nutrients on the release rate of CCK from the pools allowed for narrower peaks than the duration of the stimulatory signal. This implementation aimed to mimic the exhaustion of the CCK secretory granules contained in the pools.<sup>8</sup> The CCK pool compartments can be seen as a virtual pool of all the CCK contained in the I cells.<sup>7</sup> Fats and proteins have both been described as potent CCK secretagogues, thus the lack of support of proteins potency in the CCK model was unexpected.<sup>8,32</sup> Possibly this result could be explained by the small range of protein content (3–13 g) studied. In line with the classical statistical analysis, the covariate search revealed a significant impairment of

carbohydrate potency (–81%) in patients with T2D.<sup>17</sup> Several CCK model parameters were estimated with a high uncertainty due to model complexity and lack of data. Therefore, the reported parameters should be interpreted carefully.

CCK has been commonly described as the main factor involved in postprandial GBE.<sup>8,15</sup> Unexpectedly, while CCK plasma concentrations could to some extent predict the postprandial GBE, a lack of relationship with the nutritional content of the test drinks was observed (**Supplementary Material S4**). The present results could indicate the implication of other postprandial stimulatory factors such as neural action on the postprandial GBE.<sup>8,15</sup> The alternative model where GBE was triggered by a signal of nutrients in the duodenum yielded a simpler model structure and improved predictive performances (**Figure 2**). Unlike with the CCK model, the potency of both proteins ( $POT_{protB} = 68\%$ ) and carbohydrates ( $POT_{carbB} = 2.3\%$ ) were supported by the model and in line with previous studies.<sup>8,15</sup> The simulation-based gallbladder ejection fraction was predicted to be as high as 65%, which is consistent with studies of CCK-induced GBE.<sup>41</sup> The SCM revealed effects of WT on the  $BASE_{BILE}$  and a modest effect of age on  $S_{50-BILE}$ . These results are supported by previous publications showing a positive correlation between gallbladder volume and body size as well as a decreased gallbladder responsiveness with increasing age.<sup>42,43</sup> Future additions could be made to the developed model to predict intestinal bile acid concentrations. These concentrations could be used to more accurately predict the rate and extent of absorption of lipophilic compounds.<sup>2,5</sup>

The present model framework has been developed on test drinks and extrapolation to solid meals has yet to be tested. In addition, it was assumed that acetaminophen is emptied from the stomach at the same rate as the other nutrients; this assumption could not, however, be tested. For each crossover occasion individuals were given different test drinks, which strongly modified the kinetics of acetaminophen. Hence, it was not judged to be possible to sufficiently separate BSV from between-occasion variability based on the available data and individuals were considered independent from one occasion to another. This hypothesis was supported by the lack of high correlation of the empirical Bayes estimates between the different occasions. Finally, the nonlinear nutrient absorption parameters were scaled from published values for glucose in human.<sup>24</sup> However, a sensitivity analysis indicated that these values were not critical for the parameter estimates. The assumption was further supported by the relatively small fraction of proteins (3–13 g) and fats (2.5–40 g) studied as opposed to the large fraction of carbohydrates (25–125 g). Furthermore, the absorption rate of proteins and fats was not expected to be markedly different from the absorption of carbohydrates based on published values in mini pigs.<sup>44</sup>

In conclusion, the developed models were predictive of the postprandial changes in GE and GBE across a wide range of nutritional content. These models have the potential to improve bottom-up predictions with systems pharmacology models or to be combined with more empirical



pharmacokinetic models to better describe the postprandial changes of drug absorption.

**Acknowledgments.** This work received support from the Innovative Medicines Initiative Joint Undertaking (<http://www.imi.europa.eu>) under grant agreement number 115369, resources of which are composed of financial contribution from the European Union's Seventh Framework Programme (FP7/2007-2013) and EFPIA companies in kind contribution. The authors thank Emilie Schindler for valuable comments on the article.

**Author Contributions.** B.G., D.P.S., M.H., J.I.B., A.L., J.F.R., O.A., M.O.K., T.V., F.K.K., and M.B. wrote the article; B.G., D.P.S., M.H., J.I.B., A.L., J.F.R., O.A., M.O.K., T.V., F.K.K., and M.B. designed the research; D.P.S., M.H., and J.I.B. performed the research; B.G. analyzed the data.

**Conflict of Interest.** The authors declare no conflicts of interest.

1. Amidon, G.L., Lennemäs, H., Shah, V.P. & Crison, J.R. A theoretical basis for a biopharmaceutic drug classification: The correlation of in vitro drug product dissolution and in vivo bioavailability. *Pharm. Res. An Off. J. Am. Assoc. Pharm. Sci.* **12**, 413–420 (1995).
2. Charman, W.N., Porter, C.J., Mithani, S. & Dressman, J.B. Physicochemical and physiological mechanisms for the effects of food on drug absorption: The role of lipids and pH. *J. Pharm. Sci.* **86**, 269–282 (1997).
3. Sjögren, E. *et al.* In vivo methods for drug absorption—Comparative physiologies, model selection, correlations with in vitro methods (IVIVC), and applications for formulation/API/ excipient characterization including food effects. *Eur. J. Pharm. Sci.* **57**, 99–151 (2014).
4. Camilleri, M. Integrated upper gastrointestinal response to food intake. *Gastroenterology* **131**, 640–58 (2006).
5. Lentz, K.A. Current methods for predicting human food effect. *AAPS J.* **10**, 282–288 (2008).
6. Moran, T.H., Wirth, J.B., Schwartz, G.J. & McHugh, P.R. Interactions between gastric volume and duodenal nutrients in the control of liquid gastric emptying. *Am. J. Physiol.* **276**, R997–R1002 (1999).
7. Agersnap, M. & Rehfeld, J.F. Nonsulfated cholecystokinins in the small intestine of pigs and rats. *Peptides* **71**, 121–7 (2015).
8. Liddle, R.A. Cholecystokinins cells. *Annu. Rev. Physiol.* **59**, 221–242 (1997).
9. Kesisoglou, F., Panmai, S. & Wu, Y. Nanosizing — Oral formulation development and biopharmaceutical evaluation. *Adv. Drug Deliv. Rev.* **59**, 631–644 (2007).
10. Fleisher, D., Li, C., Zhou, Y., Pao, L. H. & Karim, A. Drug, meal and formulation interactions influencing drug absorption after oral administration. *Clinical Implications. Clin. Pharmacokinet.* **36**, 233–254 (1999).
11. Clements, J.A., Heading, R.C., Nimmo, W.S. & Prescott, L. F. Kinetics of acetaminophen absorption and gastric emptying in man. *Clin. Pharmacol. Ther.* **24**, 420–31 (1978).
12. Willems, M., Otto Quartero, A. & Numans, M.E. How useful is paracetamol absorption as a marker of gastric emptying? A systematic literature study. *Dig. Dis. Sci.* **46**, 2256–2262 (2001).
13. Raffa, R.B., Pergolizzi, J.V., Taylor, R., Decker, J.F. & Patrick, J.T. Acetaminophen (paracetamol) oral absorption and clinical influences. *Pain Pract.* **14**, 668–77 (2014).
14. Custodio, J.M., Wu, C.-Y. & Benet, L. Z. Predicting drug disposition, absorption/elimination/ transporter interplay and the role of food on drug absorption. *Adv. Drug Deliv. Rev.* **60**, 717–33 (2008).
15. Froehlich, F., Gonvers, J.J. & Fried, M. Role of nutrient fat and cholecystokinins in regulation of gallbladder emptying in man. *Dig. Dis. Sci.* **40**, 529–533 (1995).
16. Kostewicz, E.S. *et al.* PBPK models for the prediction of in vivo performance of oral dosage forms. *Eur. J. Pharm. Sci.* **57**, 300–21 (2014).
17. Sonne, D.P., Rehfeld, J.F., Holst, J.J., Vilsboll, T. & Knop, F.K. Postprandial gallbladder emptying in patients with type 2 diabetes: potential implications for bile-induced secretion of glucagon-like peptide 1. *Eur. J. Endocrinol.* **171**, 407–419 (2014).
18. Hansen, M. *et al.* Effect of chenodeoxycholic acid and the bile acid sequestrant colestyramine on glucagon-like peptide-1 secretion. *Diabetes Obes. Metab.* **18**, 571–80 (2016).
19. Bagger, J.I. *et al.* Impaired regulation of the incretin effect in patients with type 2 diabetes. *J. Clin. Endocrinol. Metab.* **96**, 737–745 (2011).
20. Sonne, D.P. *et al.* Postprandial gut hormone responses and glucose metabolism in cholecystectomized patients. *AJP Gastrointest. Liver Physiol.* **304**, 413–419 (2013).

21. Keizer, R.J., Karlsson, M.O. & Hooker, A. Modeling and simulation workbench for NONMEM: Tutorial on Pirana, PsN, and Xpose. *CPT Pharmacometrics Syst. Pharmacol.* **2**, e50 (2013).
22. Bergstrand, M. & Karlsson, M.O. Handling data below the limit of quantification in mixed effect models. *AAPS J.* **11**, 371–80 (2009).
23. Lacroix, B.D., Friberg, L.E. & Karlsson, M.O. Evaluation of IPPSE, an alternative method for sequential population PKPD analysis. *J. Pharmacokinet. Pharmacodyn.* **39**, 177–93 (2012).
24. Alskär, O. *et al.* Semimechanistic model describing gastric emptying and glucose absorption in healthy subjects and patients with type 2 diabetes. *J. Clin. Pharmacol.* **56**, 340–348 (2016).
25. Ogungbenro, K. *et al.* A semi-mechanistic gastric emptying model for the population pharmacokinetic analysis of orally administered acetaminophen in critically ill patients. *Pharm. Res.* **28**, 394–404 (2011).
26. Zuppa, A.F. *et al.* Safety and population pharmacokinetic analysis of intravenous acetaminophen in neonates, infants, children, and adolescents with pain or fever. *J. Pediatr. Pharmacol. Ther.* **16**, 246–61 (2011).
27. Gisleskog, P.O., Karlsson, M.O. & Beal, S.L. Use of prior information to stabilize a population data analysis. *J. Pharmacokinet. Pharmacodyn.* **29**, 473–505 (2002).
28. Hunt, J.N. & Stubbs, D.F. The volume and energy content of meals as determinants of gastric emptying. *J. Physiol.* **245**, 209–225 (1975).
29. Merrill, A.L. & Watt, B.K. Energy values of food: basis and derivation. *Agric. Handbook* **74**, 1–105 (1973).
30. Hénin, E., Bergstrand, M., Standing, J.F. & Karlsson, M.O. A mechanism-based approach for absorption modeling: the gastro-intestinal transit time (GITT) model. *AAPS J.* **14**, 155–63 (2012).
31. Sharma, A., Ebling, W.F. & Jusko, W.J. Precursor-dependent indirect pharmacodynamic response model for tolerance and rebound phenomena. *J. Pharm. Sci.* **87**, 1577–84 (1998).
32. Hopman, W.P., Jansen, J.B. & Lamers, C.B. Comparative study of the effects of equal amounts of fat, protein, and starch on plasma cholecystokinin in man. *Scand. J. Gastroenterol.* **20**, 843–7 (1985).
33. Monte, M.-J. Bile acids: Chemistry, physiology, and pathophysiology. *World J. Gastroenterol.* **15**, 804 (2009).
34. Datz, F., Christian, P. & Moore, J. Gender-related differences in gastric emptying. *J. Nucl. Med.* **28**, 1204–7 (1987).
35. Brogna, A. *et al.* Gastric emptying rates of solid food in relation to body mass index: An ultrasonographic and scintigraphic study. *Eur. J. Radiol.* **27**, 258–263 (1998).
36. Bonner, J.J. *et al.* Does age affect gastric emptying time? A model-based meta-analysis of data from premature neonates through to adults. *Biopharm. Drug Dispos.* **36**, 245–257 (2015).
37. Frank, J.W. *et al.* Mechanism of accelerated gastric emptying of liquids and hyperglycemia in patients with type II diabetes mellitus. *Gastroenterology* **109**, 755–65 (1995).
38. Hens, B. *et al.* Gastrointestinal transfer: in vivo evaluation and implementation in vitro and in silico predictive tools. *Eur. J. Pharm. Sci.* **63**, 233–42 (2014).
39. Calbet, J. & MacLean, D. Role of caloric content on gastric emptying in humans. *J. Physiol.* **498**, 553–559 (1997).
40. Siegel, J.A. *et al.* Biphase nature of gastric emptying. *Gut* **29**, 85–9 (1988).
41. Rohde, U. *et al.* Cholecystokinins-induced gallbladder emptying and single-dose metformin elicit additive glucagon-like peptide-1 responses. *J. Clin. Endocrinol. Metab.* **101**, 2076–2083 (2016).
42. Khalil, T. *et al.* Effect of aging on gallbladder contraction and release of cholecystokinins-33 in humans. *Surgery* **98**, 423–9 (1985).
43. Palasciano, G. *et al.* Gallbladder volume in adults, and relationship to age, sex, body mass index, and gallstones: a sonographic population study. *Am. J. Gastroenterol.* **87**, 493–7 (1992).
44. Weber, E. & Ehrlein, H.J. Composition of enteral diets and meals providing optimal absorption rates of nutrients in mini pigs. *Am. J. Clin. Nutr.* **69**, 556–563 (1999).

© 2016 The Authors CPT: Pharmacometrics & Systems Pharmacology published by Wiley Periodicals, Inc. on behalf of American Society for Clinical Pharmacology and Therapeutics. This is an open access article under the terms of the Creative Commons Attribution-NonCommercial License, which permits use, distribution and reproduction in any medium, provided the original work is properly cited and is not used for commercial purposes.

Supplementary information accompanies this paper on the CPT: Pharmacometrics & Systems Pharmacology website (<http://www.wileyonlinelibrary.com/psp4>)